

# Nonlinear modes in spatially confined spin-orbit-coupled Bose-Einstein condensates with repulsive nonlinearity

Xiong-wei Chen<sup>1,§</sup>, Zhi-gui Deng<sup>2,§</sup>, Xiao-xi Xu<sup>1,§</sup>, Shu-lan Li<sup>1</sup>,  
Zhi-wei Fan<sup>3</sup>, Zhao-pin Chen<sup>2</sup>, Bin Liu<sup>1\*</sup> and Yong-yao Li<sup>1,2</sup>

<sup>1</sup>*School of Physics and Optoelectronic Engineering, Foshan University, Foshan 528000, China*

<sup>2</sup>*Department of Physical Electronics, School of Electrical Engineering,  
Faculty of Engineering, Tel Aviv University, Tel Aviv 69978, Israel*

<sup>3</sup>*Department of Physics, University of Bath, Bath BA2 7AY, UK and*

<sup>§</sup> *These authors contributed equally to this work.*

It was found that spatially confined spin-orbit (SO) coupling, which can be induced by illuminating Bose-Einstein condensates (BECs) with a Gaussian laser beam, can help trap a spinor Bose gas in multi-dimensional space. Previous works on this topic were all based on a Boson gas featuring an attractive interaction. In this paper, we consider the trapping effect in the case in which the Boson gas features a repulsive interaction. After replacing the repulsive effect, stable excited modes of semi-vortex (SV) type and mixed-mode (MM) type, which cannot be created in a boson gas with attractive interactions, can be found in the current setting. The trapping ability and the capacity of the confined SO coupling versus the degree of the repulsive strength as well as the order of the excited mode are systematically discussed firstly through the paper. Moreover, the stability of the nonlinear mode trapped in this system with a moving reference frame is also discussed. Unlike the system with homogeneous SO coupling, two different types of stationary mobility modes can be stabilized when the SO coupling moves in the  $x$ - and  $y$ - directions, respectively. This finding indicates that the system with moving confined SO coupling features a typical anisotropic character that differs from the system with moving homogeneous SO coupling.

PACS numbers:

## I. INTRODUCTION

Spin-orbit (SO)-coupled Bose-Einstein condensates (BECs) provide an ideal and clean platform to emulate the relativistic dynamics of electrons in condensate matter physics [1–19]. Many novel phenomena, such as topological insulators, superconductors, supersolids, and the spin-Hall effect [20–23], can be simulated by BECs with SO coupling [24, 25]. Because a boson gas can feature abundant interactions, it provides many new avenues for people to reconsider these problems. Moreover, it was also reported that the SO coupling effect can help an attractive boson gas form stable matter-wave solitons in two- and three-dimensional (2D and 3D) free space [26–34]. In the area of nonlinear physics, it is well known that free-space solitons may collapse in 2D and 3D geometries via the action of the usual attractive cubic nonlinearity [35, 36]. Hence, how to stabilize solitons in multi-dimensional space remains a challenging issue. Generally, a common operation to stabilize solitons in free space beyond 1D is to modify the attractive cubic nonlinearity, which includes reducing the cubic type to the quadratic type [37, 38], changing it to the saturable nonlinearity [39], introducing a nonlocal nonlinearity [40–44], and adding competitive nonlinearities with orders different from cubic (such as the competing cubic-quintic nonlinearity [45–51]). Recently, a new type of self-bound quantum liquid, named quantum droplets, has been created from 1D to 3D space via binary BECs [52–58] and dipolar BECs [59–64] with the help of Lee-Huang-Yang (LHY) correction [65]. Quantum droplets with novel vortices in 2D space are also predicted for binary BECs assisted by the LHY term [66–68]. However, SO coupling stabilizes solitons in a different way, which are modified via a linear effect rather than a nonlinear effect. Therefore, SO coupling provides a new way for people to study solitons in multi-dimensional space.

With the help of SO coupling, families of composite matter-wave solitons, of the semi-vortex (SV) type and mixed-mode (MM) type, are created in 2D and 3D space if the spinor BECs feature an attractive interaction. Moreover, anisotropic stripe solitons and vortex solitons are created with the SV form in SO-coupled dipolar BECs [69–75]. Self-trapped modes formed by the interplay of SO coupling and the LHY term have also been considered [76–78]. In optics, spatiotemporal solitons with an SO coupling-like effect were created in planar dual-core waveguides and twisted cylinder waveguides with the self-focusing Kerr nonlinearity [79–82]. However, these solitons are all ground-

---

\*Electronic address: binliu@fosu.edu.cn

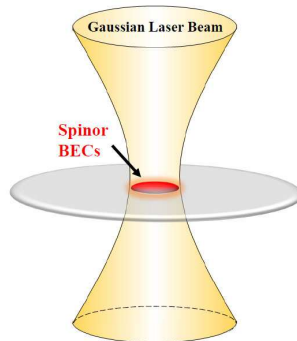


FIG. 1: (Color online) Sketch map of the model. Spinor BECs are trapped in a 2D space and illuminated by a Gaussian laser beam, which creates a spatially confined SO coupling effect.

state solutions of the system. Even though the excited-state solitons of these two types of soliton were also predicted, they are all unstable in the background of the attractive cubic nonlinearity [29]. Recent studies reveal that excited-state solitons can be stabilized if the attractive nonlinearity is replaced by the repulsive one [83]. However, such a repulsive nonlinearity cannot be homogeneous; otherwise, the self-trapped mode cannot be formed. References [84, 85] have reported that stable excited-state solitons can be found when the intensity of the local or nonlocal repulsive nonlinearity grows (with a strong growth rate) from the center. Such specific designs may bring about great difficulty in terms of experimental achievement. Hence, a natural consideration is whether the excited-state solutions can be realized under a homogeneous repulsive nonlinear background.

Very recently, it was reported that matter-wave solitons can be trapped if SO coupling, obtained under illumination by an external laser field, is applied in a spatially confined area [86–89]. This finding implies that if the strength of the SO coupling was spatially modified to be a confined one, it would be possible to achieve stable excited state modes formed via the homogeneous repulsive nonlinearity. Based on such speculation, the first objective of this paper is to demonstrate this possibility. The second objective of this paper is to verify the trapping capacity of such type of SO coupling if this possibility has been demonstrated. Then, based on the above two objectives, the final objective of this work is to consider the dynamics of these trapped modes if the SO coupling is put into a moving reference frame. Note that the stability of nonlinear modes with repulsive nonlinearity in a moving reference frame in 2D geometries has not yet been discussed. Moreover, this discussion is nontrivial because SO coupling violates Galilean invariance. To realize these targets, the rest of the paper is structured as follows. The model is introduced in Section II. Basic numerical results for the nonlinear mode in quiescent and moving reference frames are reported in Section III and IV. The paper is concluded in Section V.

## II. THE MODEL

Similar to the settings in Ref. [87], a spinor BEC is trapped by 2D SO coupling of the Rashba type within a confined area, which is illuminated by a Gaussian laser beam (see Fig.1). The illuminated area is also defined by a Gaussian function as

$$\lambda(r) = \lambda_0 \exp \left[ - \left( \frac{r}{D} \right)^2 \right],$$

where  $\lambda_0$  is the strength of the SO coupling and  $D$  stands for the size of the confined area. The mean-field model of this system is based on the Lagrangian

$$\begin{aligned} \mathcal{L} = & -\frac{i}{2} \left( \Psi_+^* \frac{\partial \Psi_+}{\partial t} + \Psi_-^* \frac{\partial \Psi_-}{\partial t} - c.c. \right) \\ & + \frac{1}{2} \left( |\nabla \Psi_+|^2 + |\nabla \Psi_-|^2 \right) + g \left[ \frac{1}{2} \left( |\Psi_+|^4 + |\Psi_-|^4 \right) + \gamma |\Psi_+|^2 |\Psi_-|^2 \right] \\ & + \frac{\lambda(r)}{2} \left\{ \left[ \Psi_+^* \frac{\partial \Psi_-}{\partial x} - \Psi_-^* \frac{\partial \Psi_+}{\partial x} - i \left( \Psi_+^* \frac{\partial \Psi_-}{\partial y} + \Psi_-^* \frac{\partial \Psi_+}{\partial y} \right) \right] + c.c. \right\}, \end{aligned} \quad (1)$$

and

$$L = \int \int \mathcal{L} dx dy, \quad (2)$$

where  $\Psi_{\pm}$  are the pseudo-spinor wave functions of the condensates, *c.c.* and the asterisk in  $\mathcal{L}$  stand for the complex conjugate, and  $g$  and  $\gamma$  are the total nonlinear strength and the relative strength of the cross-interaction, respectively. Here, the strength of the self-interaction is scaled by 1. In Ref. [87],  $g$  and  $\gamma$  are tuned to feature an attractive interaction. However, in the current setting, in order to create a stable excited mode, we replace both of them by a repulsive interaction. It's well known that the scattering length of the BEC atoms can be either positive (corresponding to a repulsive effective interaction) or negative (corresponding to an attractive one), which can be tuned by the Feshbach resonance [90–93]. The Gross-Pitaevskii equation (GPE) with the mean-field approximation can be derived from Lagrangian Eq. (2) by using the Euler-Lagrange equations as follows:

$$\begin{aligned} i \frac{\partial \Psi_+}{\partial t} &= -\frac{1}{2} \nabla^2 \Psi_+ + g \left( |\Psi_+|^2 + \gamma |\Psi_-|^2 \right) \Psi_+ + \lambda(r) \left( \frac{\partial}{\partial x} - i \frac{\partial}{\partial y} \right) \Psi_- + \frac{1}{2} e^{-i\theta} \frac{d\lambda}{dr} \Psi_-, \\ i \frac{\partial \Psi_-}{\partial t} &= -\frac{1}{2} \nabla^2 \Psi_- + g \left( |\Psi_-|^2 + \gamma |\Psi_+|^2 \right) \Psi_- - \lambda(r) \left( \frac{\partial}{\partial x} + i \frac{\partial}{\partial y} \right) \Psi_+ - \frac{1}{2} e^{i\theta} \frac{d\lambda}{dr} \Psi_+. \end{aligned} \quad (3)$$

Stationary solutions to Eqs. (3) with chemical potential  $\mu$  are sought as follows:

$$\Psi_{\pm}(\mathbf{r}, t) = \phi_{\pm}(\mathbf{r}) e^{-i\mu t}, \quad (4)$$

where  $\mathbf{r} = x\hat{\mathbf{i}} + y\hat{\mathbf{j}}$  and the functions  $\phi_{\pm}(\mathbf{r})$  satisfy the equations

$$\begin{aligned} \mu \phi_+ &= -\frac{1}{2} \nabla^2 \phi_+ + g \left( |\phi_+|^2 + \gamma |\phi_-|^2 \right) \phi_+ + \lambda(r) \left( \frac{\partial}{\partial x} - i \frac{\partial}{\partial y} \right) \phi_- + \frac{1}{2} e^{-i\theta} \frac{d\lambda}{dr} \phi_-, \\ \mu \phi_- &= -\frac{1}{2} \nabla^2 \phi_- + g \left( |\phi_-|^2 + \gamma |\phi_+|^2 \right) \phi_- - \lambda(r) \left( \frac{\partial}{\partial x} + i \frac{\partial}{\partial y} \right) \phi_+ - \frac{1}{2} e^{i\theta} \frac{d\lambda}{dr} \phi_-. \end{aligned} \quad (5)$$

The energy corresponding to Lagrangian (1) is

$$\begin{aligned} E &= \int \int (\varepsilon_K + \varepsilon_N + \varepsilon_{\text{SOC}}) dx dy, \\ \varepsilon_K &= \frac{1}{2} \left( |\nabla \phi_+|^2 + |\nabla \phi_-|^2 \right), \\ \varepsilon_N &= \frac{g}{2} \left[ \left( |\Psi_+|^4 + |\Psi_-|^4 \right) + 2\gamma |\Psi_+|^2 |\Psi_-|^2 \right], \\ \varepsilon_{\text{SOC}} &= \frac{\lambda(r)}{2} \left\{ \left[ \Psi_+^* \frac{\partial \Psi_-}{\partial x} - \Psi_-^* \frac{\partial \Psi_+}{\partial x} - i \left( \Psi_+^* \frac{\partial \Psi_-}{\partial y} + \Psi_-^* \frac{\partial \Psi_+}{\partial y} \right) \right] + c.c. \right\}, \end{aligned}$$

where  $\varepsilon_K$ ,  $\varepsilon_N$ , and  $\varepsilon_{\text{SOC}}$  are the kinetic, interaction, and SO coupling energy densities, respectively.

In the following study, we will apply the normalized condition and define the total norm as

$$N = \int \int n(\mathbf{r}) dx dy \equiv 1, \quad (6)$$

where  $n(\mathbf{r}) = |\phi_+|^2 + |\phi_-|^2$  is the effective density distribution of the nonlinear mode. Estimation of the actual number of atoms for the normalization condition on the real experiment scale can be done: if the effective length of the SO coupling is  $\sim 0.5$  m, which corresponds to a physical length of approximately  $1 \mu\text{m}$ , and  $N = 1$  corresponds to a number of atoms of  $\sim 10^4$  [87, 88].

The stationary solutions of the nonlinear mode of Eqs. (5) are solved numerically by means of the imaginary-time-integration method (ITM) [94, 95], and the stabilities of these nonlinear modes are verified via direct simulations. In the numerical simulations, we normalized  $\lambda_0 = 1$  and leave  $(D, g, \gamma)$  as a set of controlled parameters of the system.

### III. NONLINEAR MODE IN THE QUIESCENT REFERENCE FRAME

We note that Eqs. (3) admits two types of 2D stationary solutions in the form of semi-vortex (SV) modes and mixed modes (MMs). According to Refs. [84, 85], the fundamental SV modes and their excited states can be produced through the ITM by inputting the following ansatz:

$$\phi_{\pm}^{(0)} = A_{\pm} r^{S_{\pm}} \exp(-\alpha_{\pm} r^2 + i S_{\pm} \theta), \quad (7)$$

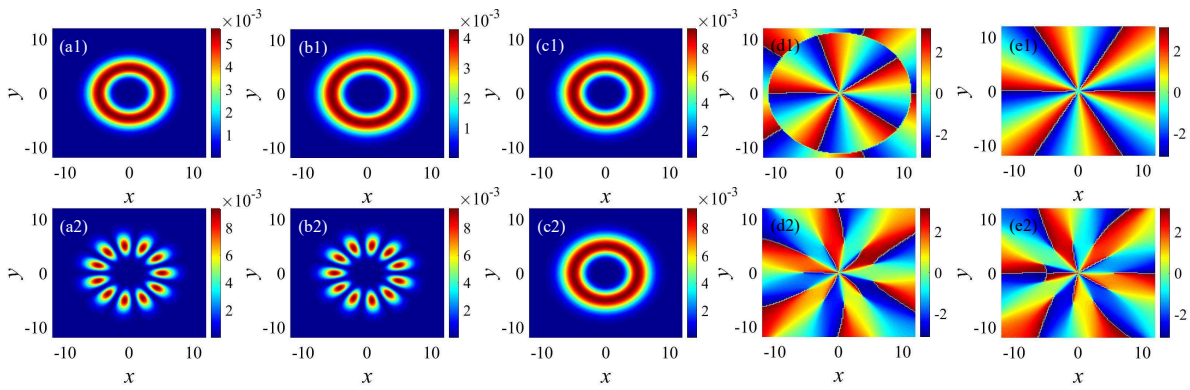


FIG. 2: (color online) (a1, b1) and (a2, b2): the density patterns of the  $\phi_+$  and  $\phi_-$  components of the excited SV and MM modes with  $S_+ = 5$  and  $S_1 = 5$ , respectively. (c1, c2): the total density patterns of the binary BEC. The fourth and fifth columns: the corresponding phase patterns of  $\phi_+$  and  $\phi_-$ . Here, we fixed parameters  $D = 10$ ,  $g = 2$  and  $\gamma = 1$ .

where  $A_{\pm}$  and  $\alpha_{\pm}$  are positive real constants and  $S_{\pm}$  is the vorticity topological charge exerted on the input. Fundamental SVs are produced by inputting  $(S_+, S_-) = (0, 1)$  or  $(-1, 0)$ , whereas excited SVs are produced by inputting  $(S_+, S_-) = (n, n + 1)$ , where  $n$  is an integer and satisfies  $n \neq -1$  or  $0$ . As for the fundamental MMs and their excited states, the ansatz is defined as

$$\phi_{\pm}^{(0)} = A_1 r^{|S_1|} \exp(-\alpha_1 r^2 \pm i S_1 \theta) \mp A_2 r^{|S_2|} \exp(-\alpha_2 r^2 \mp i S_2 \theta), \quad (8)$$

where  $A_{1,2}$  and  $\alpha_{1,2}$  are arbitrary real constants.  $S_{1,2}$  are the topological charge numbers and satisfy  $S_2 = S_1 + 1$ . Fundamental MMs can be created when  $S_1 = -1$  or  $0$ , while excited MMs are created when  $S_1$  is assigned other integer values. Because the interactions, which includes the self-interaction and the cross-interaction, in the spinor BECs are tuned to be a homogeneous repulsive interaction. As expected, stable excited SVs and MMs are found in this system. Typical examples of excited states of SVs and MMs corresponding to  $S_+ = 5$  and  $S_1 = 5$  are displayed in Fig. 2. The characteristic of these excited states are in accordance with their counterparts found in Ref. [84, 85]. However, the excited states found in previous systems, which were built via the modulation of local and nonlocal repulsion, are only stable up to  $S_1$  or  $S_+$  up to 5. In contrast, in the current system, excited modes can be found with  $S_+$  or  $S_1 > 5$  for appropriate values of the control parameters of  $(D, g, \gamma)$ . In the case of self-attractive BECs with confined SO coupling, the soliton was formed with the help not only from the confined SO coupling but also from the self-attraction [87]. Under this circumstance, the confined SO coupling does not feature a purely effect. However, in the current system, if we replace the confined SO coupling with the homogeneous SO coupling, the BECs diffuse by the repulsion. Therefore, the localized modes found in the current system purely depend on the trapping ability of the confined SO coupling. To study the dependence of the trapping ability of the confined SO coupling on the control parameters of the system, we plot the size, the chemical potential and the energy of the nonlinear mode, i.e.,  $(R, \mu, E)$ , as functions of  $(D, g, \gamma)$  in Fig. 3. Here, the size of the nonlinear mode is defined as

$$R = \left( \frac{\int \mathbf{r}^2 n(\mathbf{r}) d\mathbf{r}}{\int n(\mathbf{r}) d\mathbf{r}} \right)^{\frac{1}{2}}, \quad (9)$$

where  $n(\mathbf{r}) = |\phi_+(\mathbf{r})|^2 + |\phi_-(\mathbf{r})|^2$  is the total density distribution of the nonlinear mode. For convenience, we use the fundamental mode to characterize this dependence.

Figs. 3 (a1, a2, a3) display the size  $R$ , the chemical potential  $\mu$ , and the total energy  $E$  of fundamental SVs with  $\gamma = 1$ , respectively, as functions of the SO coupling confinement size,  $D$ , for different strengths of the repulsive interaction  $g$ . In Fig. 3(a1), the size of the nonlinear mode, which is denoted by  $R(D)$ , totally increases with increasing  $D$  when  $D > 10$ . This result indicates that the size of the nonlinear mode expands due to the repulsion if the trapping from the confined SO coupling becomes weaker. When  $D \rightarrow \infty$ , the confinement disappears, the SO coupling becomes homogeneous, and the nonlinear mode may decay to an infinite-size linear mode in 2D free space with a homogeneous SO coupling background. However, if the confined area  $D$  is too small, then it cannot provide enough area for trapping the nonlinear mode. In this circumstance, the size of the nonlinear mode starts to expand again. When  $D \rightarrow 0$ , the SO coupling disappears from the 2D space, which results in decay of the nonlinear mode to a linear mode in a purely 2D free space. Between these two limits ( $D \rightarrow 0$  and  $D \rightarrow \infty$ ), an optimized value of  $D$  appears at  $D \approx 10$ , at which the nonlinear modes are trapped with the smallest size. The existence of such an

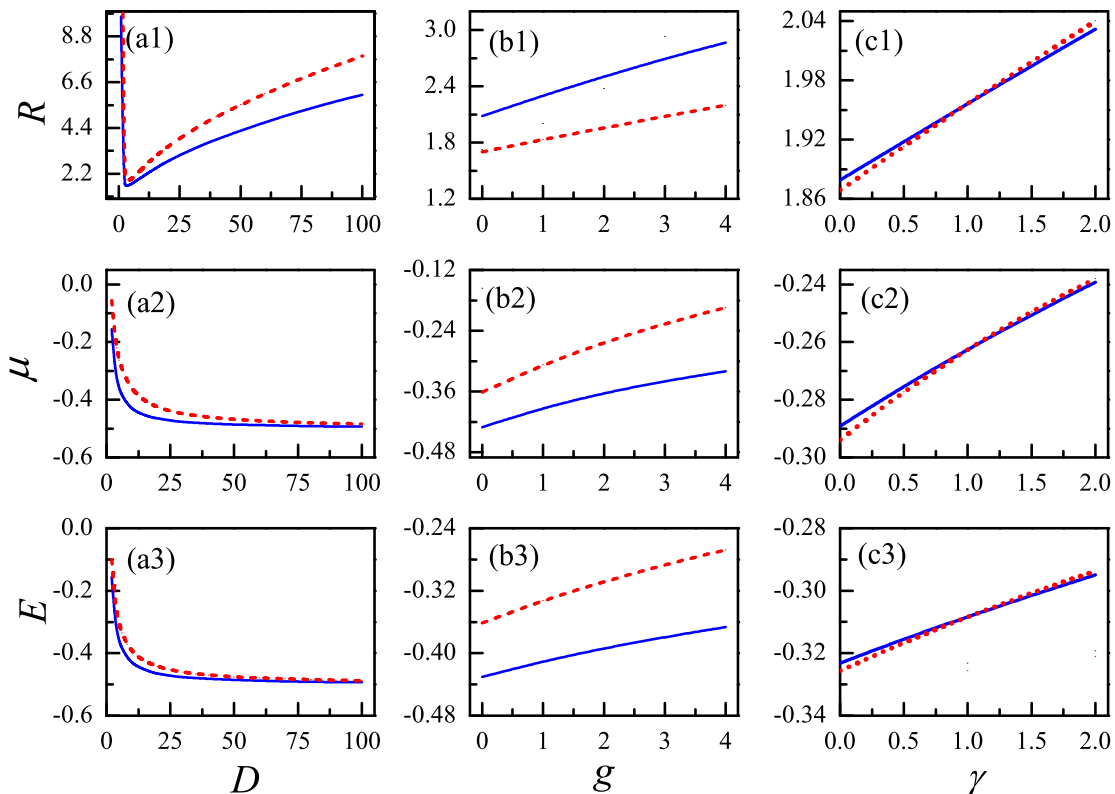


FIG. 3: (color online) The first column: the size  $R$ , the chemical potential  $\mu$ , and the total energy  $E$  of the fundamental SVs as functions of the SO coupling confinement size,  $D$ , for  $g = 0$  (the blue line) and  $g = 2$  (the red short dashed curves). The second column: the  $R$ ,  $\mu$ , and  $E$  of the fundamental SVs as functions of the total nonlinear strength,  $g$ , for  $D = 5$  (the red short dashed curves) and  $D = 10$  (the blue line). Here, we fixed  $(N, \gamma) = (1, 1)$ . The last column: the  $R$ ,  $\mu$ , and  $E$  of the SVs (the blue line) and MMs (the red short dashed curves) as functions of the strength of  $\gamma$ . Here, we fixed  $(N, g, D) = (1, 2, 10)$ .

optimized value of  $D$  is also predicted in Ref. [67]. In Figs. 3(a2, a3),  $\mu, E \rightarrow 0$  and  $-0.5$  when  $D \rightarrow 0$  and  $\infty$ , which are in accordance with the values of the chemical potential and energy of the linear mode in 2D free space with and without a homogeneous SO coupling background [27].

Figs. 3(b1, b2, b3) display the  $(R, \mu, E)$  of fundamental SVs as functions of  $g$  with  $\gamma = 1$  and different values of  $D$ . The dependence between these characters and  $g$  can be naturally understood. Fig. 3(b1) indicates that an increase in the strength of the repulsion of BECs may increase the size of the nonlinear mode. Figs. 3(b2, b3) imply that the functions of  $\mu(g)$  and  $E(g)$  satisfy the anti-VK (Vakhitov-Kolokolov) criterion, which is a necessary stability condition for nonlinear modes with a repulsive interaction [96].

Finally, Fig. 3 (c1, c2, c3) present the  $(R, \mu, E)$  of the two types of nonlinear modes, fundamental SVs and MMs, as functions of  $\gamma$  for fixed values of  $D$  and  $g$ . The figures show that these functions all increase with increasing  $\gamma$ .  $(R, \mu, E)_{\text{MM}}$  is smaller or greater than  $(R, \mu, E)_{\text{SV}}$  when  $\gamma < 1$  or  $\gamma > 1$ , respectively. Hence, intersections are found between the functions for SVs and MMs at  $\gamma = 1$ . This finding shows that SVs and MMs are degenerate at this point, which is the same finding as that in previous works [27, 85]: the SVs and MMs are degenerate under the condition of a Manakov type [97]. This result also explains why we can use SVs with  $\gamma = 1$  to identify the characteristics of the confined SO coupling in Figs. 3 (a1, a2, a3) and (b1, b2, b3).

The above discussion on the characteristics of the confined SO coupling was based on the fundamental mode. Because this system supports the existence of the excited mode, a nontrivial discussion related to the capacity of the confined SO coupling for the excited modes needs to be addressed by the current paper. Because the excited SVs and MMs are also degenerate at  $\gamma = 1$ , which is the same as their fundamental counterparts, we will adopt excited SVs with  $\gamma = 1$  in the following discussion for convenience. The excited modes in this system are characterized by the topological number (i.e.,  $S_+$  for excited SVs or  $S_1$  for excited MMs). Fig. 4(a) shows that the size of the total density pattern of the excited SVs and MMs increases with the number of positive  $S_+$  and  $S_1$ . The complete overlap of  $R(S_+)$  and  $R(S_1)$  demonstrates the validity of using excited SVs to represent excited MMs at  $\gamma = 1$  to study the

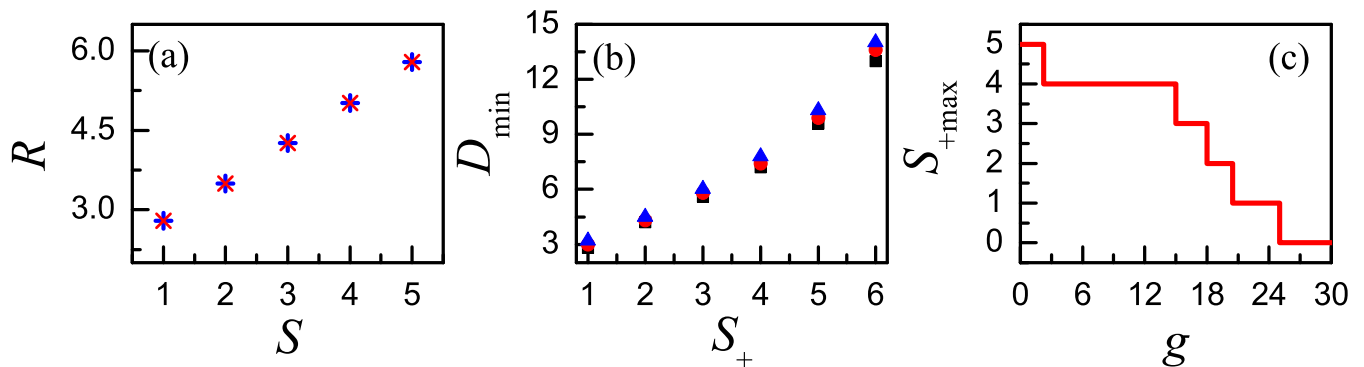


FIG. 4: (color online) (a) The size of the total density pattern of the excited SVs (marked with “ $\times$ ” symbols) and MMs (marked with “+” symbols) with different topological number  $S$ ; here,  $(N, g, D) = (1, 2, 10)$ . (b) The dependence of the minimum SO coupling confinement size,  $D_{\min}$ , on the topological number  $S_+$  for different repulsive strengths  $g$  ( $g = 0$  for solid black squares,  $g = 2$  for solid red circles and  $g = 4$  for solid blue triangles). (c) The trapping ability for the maximum topological number  $S_{+\max}$  versus the degree of the nonlinear strength  $g$ ; here,  $(N, \gamma, D) = (1, 1, 10)$ .

capacity of the confined SO coupling for the excited modes.

Numerical studies find that there is a minimum area, i.e., a threshold of confined area, for the SO coupling confinement, namely,  $D_{\min}$ , for excited modes with different values of  $S_+$ . Fig. 4(b) shows the dependence of  $D_{\min}$  on the charge number  $S_+$  for different values of  $g$ . When  $D > D_{\min}(S_+)$ , a stable excited state with charge number  $S_+$  can be found in the system. When  $D < D_{\min}(S_+)$ , an excited mode with charge number  $S_+$  cannot exist in the system. The numerical simulation shows that all the inputs with charge number greater than  $S_+$  converge to the fundamental mode. Fig. 4(b) indicates that  $D_{\min}(S_+)$  increases as  $S_+$  and  $g$  increase, which can be naturally understood because higher excited modes with larger values of  $g$  require larger thresholds for the confined area because they possess larger values of  $R$ . On the other hand, Fig. 4(b) can also be applied to estimate the number of excited modes trapped by the confined SO coupling. For example, if we select  $g = 2$  and  $D = 10$ , which satisfies  $D > D_{\min}(S_+ = 5)$ , such a confined area can contain the excited mode with topological number up to  $S_+ = 5$ . According to this application, for a fixed value of  $D$ , there is a maximum topological number  $S_{+\max}$ , which denotes the number of excited modes existing in this setting. Hence,  $S_{+\max}$  can be used to identify the capacity of confined SO coupling with a fixed value of  $D$ . Fig. 4(c) manifests the dependence of the maximum topological number  $S_{+\max}$  and the repulsive strength  $g$  for a fixed value of  $D$ . As discussed above, since an increase in  $g$  can expand the size of the excited nonlinear mode, one can see that the capacity of the confined SO coupling decreases with increasing  $g$ .

#### IV. NONLINEAR MODE IN CONFINED SO COUPLING WITH A MOVING REFERENCE FRAME

Unlike the usual system without SO coupling, a system with SO coupling does not obey Galilean invariance. Hence, studying the mobility of the nonlinear mode is another nontrivial issue for a system with SO coupling. Reference [27] reported that only one type of stable nonlinear mode was found when the system only moves in the  $y$  direction up to a threshold velocity. For the current system, we will demonstrate that more than one type of stable nonlinear mode can be found; additionally, a nonlinear mode can be found to be stable when the system moves in the  $x$  direction.

Here, we assume stable transfer of the nonlinear mode by the moving SO coupling profile, which corresponds to

$$\begin{aligned}
 (x', y') &\rightarrow (x - v_x t, y - v_y t), \\
 \lambda'(r') &\rightarrow \lambda(r), \\
 \tilde{\Psi}_{\pm}(\mathbf{r}', t) &= \Psi_{\pm}(\mathbf{r}, t), \\
 \Psi'_{\pm}(\mathbf{r}', t) &= \tilde{\Psi}_{\pm}(\mathbf{r}', t) \exp \left[ \frac{i}{2} (v_x x'^2 + v_y y'^2) \right].
 \end{aligned} \tag{10}$$

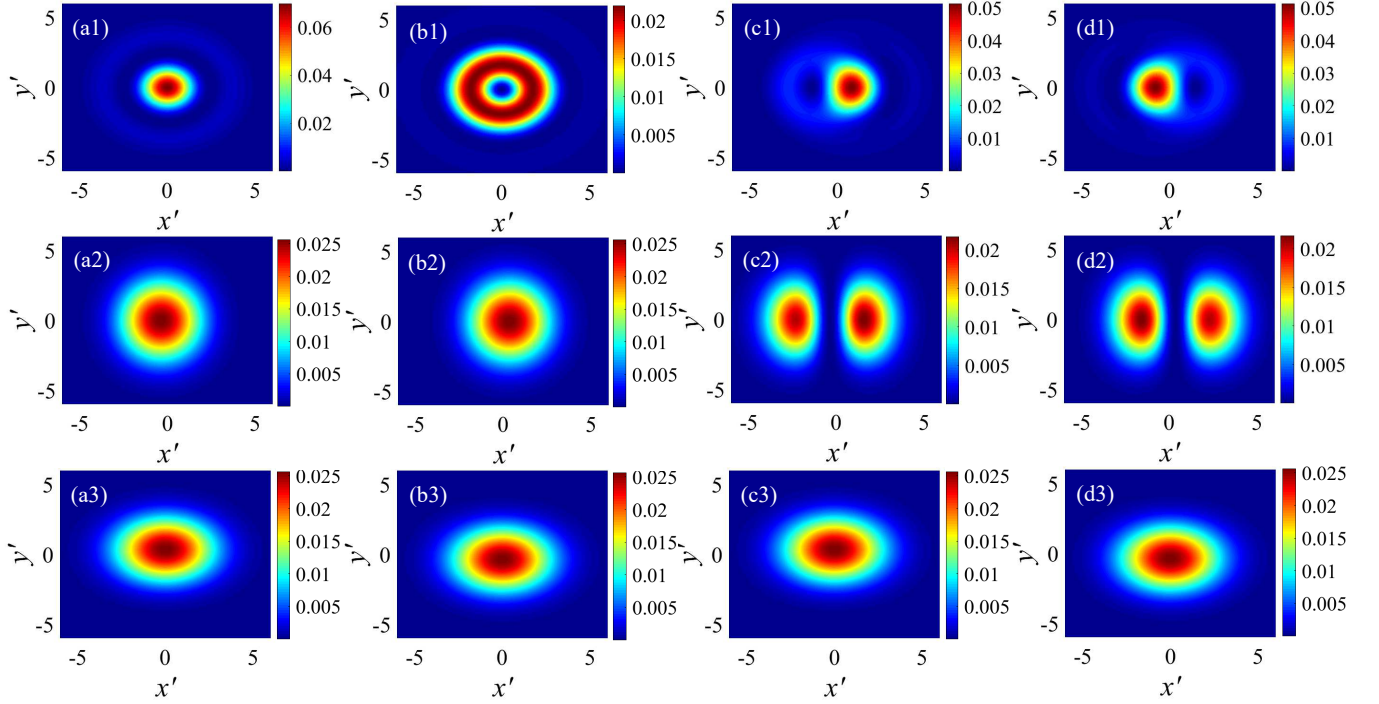


FIG. 5: (Color online) Density distribution of the nonlinear mode in the moving reference frame. Figs. (a1, b1, c1, d1) shows the system with  $v_x = v_y = 0$ , and Figs. (a2, b2, c2, d2) shows the system moving in the  $y$ -direction with  $v_x = 0$  and  $v_y = 0.5$ . Figs. (a3, b3, c3, d3) shows the system moving in the  $x$ -direction with  $v_x = 0.5$  and  $v_y = 0$ . The first through fourth columns present the density distribution for each component obtained by inputting an SV guess and an MM guess into Eqs. (7) and (8), respectively. Here, we fixed  $(D, \gamma, g) = (10, 1, 2)$ .

Eqs. (3) are transformed into the following forms:

$$\begin{aligned}
 i \frac{\partial \Psi'_+}{\partial t} &= -\frac{1}{2} \nabla'^2 \Psi'_+ + g \left( |\Psi'_+|^2 + \gamma |\Psi'_-|^2 \right) \Psi'_+ + \lambda' \left( \frac{\partial}{\partial x'} - i \frac{\partial}{\partial y'} \right) \Psi'_- + \frac{e^{-i\theta'}}{2} \frac{d\lambda'}{dr'} \Psi'_- + \lambda'(r') (iv_x + v_y) \Psi'_-, \\
 i \frac{\partial \Psi'_-}{\partial t} &= -\frac{1}{2} \nabla'^2 \Psi'_- + g \left( |\Psi'_-|^2 + \gamma |\Psi'_+|^2 \right) \Psi'_- - \lambda' \left( \frac{\partial}{\partial x'} + i \frac{\partial}{\partial y'} \right) \Psi'_+ - \frac{e^{i\theta'}}{2} \frac{d\lambda'}{dr'} \Psi'_+ - \lambda'(r') (iv_x - v_y) \Psi'_+. \quad (11)
 \end{aligned}$$

Obviously, the last term in Eqs. (11), which is modulated by  $\lambda'(r')$ , makes the nonlinear modes in the current system differ from their counterparts in the system with homogeneous SO coupling.

Here, a stationary solution in the moving reference frame is obtained by solving Eqs. (11) by means of the ITM. The stabilities of the solution are checked via direct simulation using Eqs. (11). The inputs still adopt the definitions in Eqs. (7) and (8) for the two types of nonlinear modes. For convenience, we will fix  $D = 10$  and  $\gamma = 1$  in this section. Typical examples of the stable nonlinear modes, which are generated by inputting Eqs. (7) and (8) with  $S_+ = S_1 = 0$ , for states with different values of  $v_x$  and  $v_y$  are displayed in Fig. 5.

In the limit of  $v_x = v_y = 0$ , which is the same as the system in the quiescent reference frame, as expected, stable fundamental SV modes and MMs are generated by inputting different types of guesses. However, once  $v_x$  or  $v_y$  differ from 0, only nonlinear modes with

$$N_+ = \int |\Psi'_+(\mathbf{r}')|^2 d\mathbf{r}' = \int |\Psi'_-(\mathbf{r}')|^2 d\mathbf{r}' = N_-$$

are found in the system. In the case of  $v_y \neq 0$  and  $v_x = 0$ , two types of stationary modes are found by inputting two types of guesses. The SV guess in Eq. (7) produces a single hump profile density distribution for each component. The density distributions of the two components deviating from the axis of  $x' = 0$  feature a mirror symmetry about this axis, which is similar to the findings of nonlinear modes in the mobility system with  $v_y \neq 0$  in Refs. [27] and [77]. In contrast, the MM guess in Eq. (8) generates a stable nonlinear mode different from the counterpart produced by the SV guess. The density distributions of such nonlinear modes have a double-hump structure. The center between

the two humps is exactly located at the axis of  $x' = 0$ . Typical examples of these two types of nonlinear modes are displayed in the second row of Fig. 5. Finally, in the case of  $v_x \neq 0$  and  $v_y = 0$ , only one type of nonlinear mode can be produced regardless of whether an SV guess or an MM guess are input. The density distribution of this nonlinear mode has a single hump structure. It is similar to the nonlinear mode produced by the SV guess in the case of  $v_x = 0$  and  $v_y \neq 0$ , whereas its mirror symmetry axis changes to  $y' = 0$ . Typical examples of this type of nonlinear mode are shown in the third row of Fig. 5.

The system with homogeneous SO coupling (refer to Ref. [27]), which presented the stable MM moves only in the  $y$  direction up to a threshold velocity and the SV mode is hardly moving. In our system, we find different types of stationary mobility modes when the moving velocity is along the  $x$  and  $y$  directions. In the case of moving along the  $y$  direction, two types of nonlinear modes can be found by inputting different types of guesses, while in the case of moving along the  $x$  direction, only one type of nonlinear mode can be found regardless of what type of guess is input. This result reveals that the anisotropic moving characteristics for the confined 2D SO coupling, which are different from the counterpart produced for the homogeneous SO coupling.

## V. CONCLUSION

The objective of this work is to construct several types of self-trapping nonlinear modes in the 2D model of binary Bose-Einstein condensates (BECs) with a repulsive interaction and spatially confined spin-orbit (SO) coupling. Spatially confined SO coupling can be induced in spinor BECs by illuminating them with a Gaussian laser beam. Such a confined effect can make the SO coupling feature a trapping capacity for the nonlinear mode. The most essential finding is that compared to the attractive interaction, excited semi-vortex (SV) modes and mixed modes (MMs) with higher topological charge numbers can be stabilized by the confined SO coupling in this setting. The trapping ability versus the degree of the repulsive strength as well as the topological charge number are systematically identified in the paper. The minimum SO coupling confined size,  $D_{min}$ , is found for excited modes with different topological charge numbers and different strengths of repulsion. A nontrivial discussion on the capacity of the SO coupling with fixed confined size, which defines how many excited modes can be contained in this confined area, is presented in the paper. Another nontrivial discussion on the stability of the nonlinear modes in a moving system is also considered. We find that different types of stationary mobility modes can be stabilized when the SO coupling moves in the  $x$ - and  $y$ -directions. This finding indicates that the system with moving confined SO coupling features a different anisotropic character compared to its counterpart with moving homogeneous SO coupling.

## VI. ACKNOWLEDGMENTS

This work was supported by NNSFC (China) through grant Nos. 11905032, 11874112, and 11575063, the Foundation for Distinguished Young Talents in Higher Education of Guangdong through grant Nos. 2018KQNCX279 and 2018KQNCX009, and the Special Funds for the Cultivation of Guangdong College Students Scientific and Technological Innovation, No. pdjh2019b0514.

### Compliance with ethical standards

**Conflict of interest** The authors have declared that no conflict of interest exists.

**Ethical standards** This Research does not involve Human Participants and/or Animals.

- 
- [1] Stanescu, T.D., Anderson, B., Galitski, V.: Spin-orbit coupled Bose-Einstein condensates, *Phys. Rev. A* **78**, 023616 (2008).
  - [2] Lin, Y.J., Jiménez-García, K., Spielman, I.B.: Spin-orbit-coupled Bose-Einstein condensates, *Nature*, **471**, 83 (2011).
  - [3] Wu, Z., Zhang, L., Sun, W., Xu, X., Wang, B., Ji, S., Deng, Y., Chen, S., Liu, X., Pan, J.: Realization of two-dimensional spin-orbit coupling for Bose-Einstein condensates, *Science*, **354**, 83(2016).
  - [4] Deng, Y., Cheng, J., Jing, H., Sun, C.-P., and Yi, S.: Spin-Orbit-Coupled Dipolar Bose-Einstein Condensates, *Phys. Rev. Lett.* **108**, 125301 (2012).
  - [5] Huang, L., Meng, Z., Wang, P., Peng, P., Zhang, S., Chen, L., Li, D., Zhou, Q. and Zhang, J.: Experimental realization of two-dimensional synthetic spin-orbit coupling in ultracold Fermi gases, *Nat. Phys.* **12**, 540 (2016).
  - [6] Zhang, Y., Mao, L., and Zhang, C.: Mean-Field Dynamics of Spin-Orbit Coupled Bose-Einstein Condensates, *Phys. Rev. Lett.* **108**, 035302 (2012).
  - [7] Li, Y., Martone, G.I., Pitaevskii, L.P., Stringari, S.: Superstripes and the Excitation Spectrum of a Spin-Orbit-Coupled Bose-Einstein condensate, *Phys. Rev. Lett.* **110**, 235302 (2013).

- [8] Xu, Y., Zhang, Y., and Wu, B.: Bright solitons in spin-orbit coupled Bose-Einstein condensates, *Phys. Rev. A* **87**, 013614 (2013).
- [9] Zhang, R.F., Zhang, X.F., Li, L.: Exotic vortex structures of the dipolar Bose-Einstein condensates trapped in harmonic-like and toroidal potential, *Physics Letters A* **383**, 231 (2019).
- [10] Zhang, R.F., Zhang, Y., Li, L.: Ground states of spin-orbit-coupled Bose Einstein condensates in the presence of external magnetic field, *Physics Letters A* **383**, 3175 (2019).
- [11] Wen, L., Liang, Y., Zhou, J., Yu, P., Xia, L., Niu, L., Zhang, X.: Effects of linear Zeeman splitting on the dynamics of bright solitons in spin-orbit coupled Bose-Einstein condensates, *Acta Physica Sinica* **68**, 080301 (2019).
- [12] Wen, L., Sun, Q., Wang, H.Q., Ji, A.C., and Liu, W.M.: Ground state of spin-1 Bose-Einstein condensates with spin-orbit coupling in a Zeeman field, *Phys. Rev. A* **86**, 043602 (2012).
- [13] Wen, L., Zhang, X., Hu, A., Zhou, J., Yu, P., Xia, L., Sun, Q., Ji, A.-C.: Dynamics of bright-bright solitons in Bose-Einstein condensate with Raman-induced one-dimensional spin-orbit coupling, *Annals of Physics* **390**, 180 (2018).
- [14] Han, W., Zhang, X.F., Wang, D.S., Jiang, H.F., Zhang, W., and Zhang, S.G.: Chiral Supersolid in Spin-Orbit-Coupled Bose Gases with Soft-Core Long-Range Interactions, *Phys. Rev. Lett.* **121**, 030404 (2018).
- [15] Zhang, X.F., Kato, M., Han, W., Zhang, S.G., and Saito, H.: Spin-orbit-coupled Bose-Einstein condensates held under a toroidal trap, *Phys. Rev. A* **95**, 033620 (2017).
- [16] Peng, P., Li, G.Q., Zhao, L.C., Yang, W.L., Yang, Z.Y.: Magnetized vector solitons in a spin-orbit coupled spin-1 Bose-Einstein condensate with Zeeman coupling, *Physics Letters A* **383**, 2883 (2019).
- [17] Wang, J.G., Wang, W., Bai, X.D., and Yang, S.J.: Ring phases of spin-orbit coupled Bose-Einstein condensate in the radial optical lattices, *Eur. Phys. J. Plus* **27**, 134 (2019).
- [18] Wang, L.X., Dai, C.Q., Wen, L., Liu, T., Jiang, H.F., Saito, H., Zhang, Sh.G., and Zhang, X.F., Dynamics of vortices followed by the collapse of ring dark solitons in a two-component Bose-Einstein condensate, *Phys. Rev. A* **97**, 063607 (2018).
- [19] Liu, B., Zhong, R., Chen, Zh., Qin, X., Zhong, H., Li, Y., and Malomed, B.A., Holding and transferring matter-wave solitons against gravity by spin-orbit-coupling tweezers, *New J. Phys.* **22**, 043004 (2020).
- [20] Hasan, M.Z. and Kane, C.L.: Colloquium: Topological insulators, *Rev. Mod. Phys.* **82**, 3045 (2010).
- [21] Qi, X.L., and Zhang, S.C.: Topological insulators and superconductors. *Rev. Mod. Phys.* **83**, 1057 (2011).
- [22] Li, J., Lee, J., Huang, W., Burchesky, S., Shteynas, B., Top, F.C., Jamison, A.O., Ketterle, W.: A stripe phase with supersolid properties in spin-orbit-coupled Bose-Einstein condensates, *Nature*, **543**, 91 (2017).
- [23] Stuhl, B.K., Lu, H.-I., Ayccock, L.M., Genkina, D., Spielman, I.B.: Visualizing edge states with an atomic Bose gas in the quantum Hall regime, *Science*, **349**, 1514(2015).
- [24] Zhai, H.: Degenerate quantum gases with spin-orbit coupling: a review, *Rep. Prog. Phys.* **78**, 026001(2015).
- [25] Zhang, Y., Mossman, M.E., Busch, T., Engels, P., Zhang, C.: Properties of spin-orbit-coupled Bose-Einstein condensates, *Front. Phys.* **11**, 118103 (2016).
- [26] Lobanov, V.E., Kartashov, Y.V., Konotop, V.V.: Fundamental, Multipole, and Half-Vortex Gap Solitons in Spin-Orbit Coupled Bose-Einstein condensates, *Phys. Rev. Lett.* **112**, 180403 (2014).
- [27] Sakaguchi, H., Malomed, B.A.: Creation of two-dimensional composite solitons in spin-orbit-coupled self-attractive Bose-Einstein condensates in free space, *Phys. Rev. E* **89**, 032920 (2014).
- [28] Sakaguchi, H., Sherman, E.Y., Malomed, B.A.: Vortex solitons in two-dimensional spin-orbit coupled Bose-Einstein condensates: Effects of the Rashba-Dresselhaus coupling and Zeeman splitting, *Phys. Rev. E* **94**, 032202 (2016).
- [29] Sakaguchi, H., Malomed, B.A.: One- and two-dimensional gap solitons in spin-orbit-coupled systems with Zeeman splitting, *Phys. Rev. A* **97**, 013607 (2018).
- [30] Malomed, B.A.: Creating solitons by means of spin-orbit coupling, *Europhys. Lett.* **122**, 36001 (2018).
- [31] Chen, G., Liu, Y., Huang, H.: Mixed-mode solitons in quadrupolar BECs with spin-orbit coupling, *Commun. Nonlinear Sci. Numer. Simulat.* **48**, 318 (2017).
- [32] Gautam, S., and Adhikari, S.K.: Vortex-bright solitons in a spin-orbit-coupled spin-1 condensate, *Phys. Rev. A* **95**, 013608 (2017).
- [33] Sakaguchi, H., Malomed, B.A.: Nonlinear Management of Topological Solitons in a Spin-Orbit-Coupled System, *Symmetry*, **11**, 388 (2019).
- [34] Zhang, Y., Zhou, Z., Malomed, B.A., and Pu, H.: Stable Solitons in Three-Dimensional Free Space without the Ground State: Self-Trapped Bose-Einstein Condensates with Spin-Orbit Coupling, *Phys. Rev. Lett.* **115**, 253902 (2015).
- [35] Malomed, B.A., Mihalache, D., Wise, F., and Torner, L.: Spatiotemporal optical solitons, *J. Opt. B* **7**, R53 (2005).
- [36] Bergé, L.: Wave collapse in physics: Principles and applications to light and plasma waves, *Phys. Rep.* **303**, 259 (1998).
- [37] Torruellas, W.E., Wang, Z., Hagan, D.J., VanStryland, E.W., Stegeman, G.I., Torner, L., and Menyuk, C.R.: Observation of Two-Dimensional Spatial Solitary Waves in a Quadratic Medium, *Phys. Rev. Lett.* **74**, 5036 (1995).
- [38] Liu, X., Beckwitt, K., and Wise, F.: Two-dimensional optical spatiotemporal solitons in quadratic media, *Phys. Rev. E* **62**, 1328 (2000).
- [39] Segev, M., Valley, G.C., Crosignani, B., DiPorto, P., and Yariv, A.: Steady-State Spatial Screening Solitons in Photorefractive Materials with External Applied Field, *Phys. Rev. Lett.* **73**, 3211 (1994).
- [40] Peccianti, M., Brzdakiewicz, K.A., and Assanto, G.: Nonlocal spatial soliton interactions in nematic liquid crystals, *Opt. Lett.* **27** 1460 (2002).
- [41] Pedri, P., and Santos, L.: Two-Dimensional Bright Solitons in Dipolar Bose-Einstein Condensates, *Phys. Rev. Lett.* **95**, 200404 (2005).
- [42] Tikhonenkov, I., Malomed, B.A., and Vardi, A.: Anisotropic Solitons in Dipolar Bose-Einstein Condensates, *Phys. Rev.*

- Let. **100**, 090406 (2008).
- [43] Huang, J., Jiang, X., Chen, H., Fan, Z., Pang, W., and Li, Y.: Quadrupolar matter-wave soliton in two-dimensional free space, *Front. Phys.* **10**, 100507 (2015).
- [44] Maucher, F., Henkel, N., Saffman, M., Królikowski, W., Skupin, S., and Pohl, T.: Rydberg-Induced Solitons: Three-Dimensional Self-Trapping of Matter Waves, *Phys. Rev. Lett.* **106**, 170401 (2011).
- [45] Mihalache, D., Mazilu, D., Crasovan, L.-C., Malomed, B.A., and Lederer, F.: Three-dimensional spinning solitons in the cubic-quintic nonlinear medium, *Phys. Rev. E* **61**, 7142 (2001).
- [46] Konar, S., Mishra, M., Jana, S.: Nonlinear evolution of cosh-Gaussian laser beams and generation of flat top spatial solitons in cubic quintic nonlinear media, *Phys. Lett. A* **362**, 505 (2007).
- [47] Falcão-Filho, E.L., Araújo, C.B.de, Boudebs, G., Leblond, H., and Skarka, V.: Robust Two-Dimensional Spatial Solitons in Liquid Carbon Disulfide, *Phys. Rev. Lett.* **110**, 013901 (2013).
- [48] Wang, Y.Y., Chen, L., Dai, C.Q., Zheng, J., Fan, Y.: Exact vector multipole and vortex solitons in the media with spatially modulated cubic-quintic nonlinearity, *Nonlinear Dyn* **90**, 1269 (2017).
- [49] Dai, C.Q., Chen, R.P., Wang, Y.Y., Fan, Y.: Dynamics of light bullets in inhomogeneous cubic-quintic-septimal nonlinear media with PT-symmetric potentials, *Nonlinear Dyn* **87**, 1675-1683 (2017).
- [50] Chen, Y., Zheng, L., Xu, F., Spatiotemporal vector and scalar solitons of the coupled nonlinear Schrödinger equation with spatially modulated cubic-quintic-septimal nonlinearities, *Nonlinear Dyn* **93**, 2379-2388 (2018).
- [51] Li, J., Zhu, Y., Han, J., Qin, W., Dai, C., Wang, S., Scalar and vector multipole and vortex solitons in the spatially modulated cubic-quintic nonlinear media, *Nonlinear Dyn* **91**, 757-765 (2018).
- [52] Petrov, D.S.: Quantum Mechanical Stabilization of a Collapsing Bose-Bose Mixture, *Phys. Rev. Lett.* **115**, 155302 (2015)
- [53] Petrov, D.S., and Astrakharchik, G. E.: Ultradilute Low-Dimensional Liquids, *Phys. Rev. Lett.* **117**, 100401 (2016).
- [54] Cabrera, C.R., Tanzi, L., Sanz, J., Naylor, B., Thomas, P., Cheiney, P., Tarruell, L.: Quantum liquid droplets in a mixture of Bose-Einstein condensates, *Science* **359**, 301 (2018).
- [55] Liu, B., Zhang, H., Zhong, R., Zhang, X., Qin, X., Huang, X., Li, Y., Malomed, B.A.: Symmetry breaking of quantum droplets in a dual-core trap, *Phys. Rev. A*, **99**, 053602 (2019).
- [56] Kartashov, Y.V., Malomed, B.A., and Torner, L.: Metastability of Quantum Droplet Clusters, *Phys. Rev. Lett.* **122**, 193902 (2019).
- [57] Zhou, Z., Yu, X., Zou, Y., Zhong, H.: Dynamics of quantum droplets in a one-dimensional optical lattice, *Commun. Nonlinear Sci. Numer. Simulat.* **67**, 617(2019).
- [58] Astrakharchik, G.E. and Malomed, B.A.: Dynamics of onedimensional quantum droplets, *Phys. Rev. A* **98**, 013631 (2018).
- [59] Schmitt, M., Wenzel, M., Böttcher, F., Ferrier-Barbut, I., and Pfau, T.: Self-bound droplets of a dilute magnetic quantum liquid, *Nature* **539**, 259 (2016).
- [60] Chomaz, L., Baier, S., Petter, D., Mark, M. J., Wächtler, F., Santos, L., and Ferlaino, F.: Quantum-Fluctuation-Driven Crossover from a Dilute Bose-Einstein Condensate to a Macrodroplet in a Dipolar Quantum Fluid, *Phys. Rev. X* **6**, 041039 (2016).
- [61] Baillie, D., Wilson, R.M., Bisset, R.N., and Blakie, P.B.: Self-bound dipolar droplet: A localized matter wave in free space, *Phys. Rev. A* **94**, 021602(R) (2016).
- [62] Wächtler, F., and Santos, L.: Ground-state properties and elementary excitations of quantum droplets in dipolar Bose-Einstein condensates, *Phys. Rev. A* **94**, 043618 (2016).
- [63] Ferrier-Barbut, I., Kadau, H., Schmitt, M., Wenzel, M., and Pfau, T.: Observation of Quantum Droplets in a Strongly Dipolar Bose Gas, *Phys. Rev. Lett.* **116**, 215301 (2016).
- [64] Edler, D., Mishra, C., Wächtler, F., Nath, R., Sinha, S., and Santos, L.: Quantum Fluctuations in Quasi-One-Dimensional Dipolar Bose-Einstein Condensates, *Phys. Rev. Lett.* **119**, 050403 (2017).
- [65] Lee, T.D., Huang, K.S., and Yang, C.N.: Eigenvalues and eigenfunctions of a Bose system of hard spheres and Its Low-temperature properties, *Phys. Rev.* **106**, 1135(1957).
- [66] Li, Y., Chen, Z., Luo, Z., Huang, C., Tan, H., Pang, W., and Malomed, B.A.: Two-dimensional vortex quantum droplets, *Phys. Rev. A* **98**, 063602 (2018).
- [67] Zhang, X., Xu, X., Zheng, Y., Chen, Z., Liu, B., Huang, C., Malomed, B.A., and Li, Y.: Semidiscrete Quantum Droplets and Vortices, *Phys. Rev. Lett.* **123**, 133901 (2019).
- [68] Tengstrand, M.N., Stürmer, P., Karabulut, E.Ö., and Reimann, S.M.: Rotating Binary Bose-Einstein Condensates and Vortex Clusters in Quantum Droplets, **123**, 160405 (2019).
- [69] Xu, Y., Zhang, Y., and Zhang, C.: Bright solitons in a two-dimensional spin-orbit-coupled dipolar Bose-Einstein condensate, *Phys. Rev. A* **92**, 013633 (2015).
- [70] Jiang, X., Fan, Z., Chen, Z., Pang, W., Li, Y., and Malomed, B.A.: Two-dimensional solitons in dipolar Bose-Einstein condensates with spin-orbit coupling, *Phys. Rev. A* **93**, 023633 (2016).
- [71] Li, Y., Liu, Y., Fan, Z., Pang, W, Fu, S., and Malomed, B.A.: Two-dimensional dipolar gap solitons in free space with spin-orbit coupling, *Phys. Rev. A* **95**, 063613 (2017).
- [72] Liao, B., Li, S., Huang, C., Luo, Z., Pang, W., Tan, H., Malomed, B.A., and Li, Y.: Anisotropic semivortices in dipolar spinor condensates controlled by Zeeman splitting, *Phys. Rev. A* **96**, 043613 (2017).
- [73] Liao, B., Ye, Y., Zhuang, J., Huang, C., Deng, H., Pang, W., Liu, B., Li, Y.: Anisotropic solitary semivortices in dipolar spinor condensates controlled by the two-dimensional anisotropic spin-orbit coupling, *Chaos, Solitons and Fractals*, **116**, 424 (2018).
- [74] Liu, S., Liao, B., Kong, J., Chen, P., Lü, J., Li, Y., Huang, C., and Li, Y.: Anisotropic Semi Vortices in Spinor Dipolar

- Bose Einstein Condensates Induced by Mixture of Rashba Dresselhaus Coupling, *J. Phys. Soc. Jpn.* **87**, 094005 (2018).
- [75] Pang, W., Deng, H., Liu, B., Xu, J., and Li, Y.: Two-Dimensional Vortex Solitons in Spin-Orbit-Coupled Dipolar Bose-Einstein Condensates, *Applied Science*, **8**, 1771(2018).
- [76] Cui, X.: Spin-orbit-coupling-induced quantum droplet in ultracold Bose-Fermi mixtures, *Phys. Rev. A* **98**, 023630 (2018).
- [77] Li, Y., Luo, Z., Liu, Y., Chen, Z., Huang, C., Fu, S., Tan, H., and Malomed, B.A.: Two-dimensional solitons and quantum droplets supported by competing self- and cross-interactions in spin-orbit-coupled condensates, *New J. Phys.* **19**, 113043(2017).
- [78] Sahu, S., Majumder, D.: Collective excitations of two-dimensional Bose-Einstein Condensate in liquid phase with spin-orbit coupling, arXiv: 1910.00264.
- [79] Kartashov, Y.V., Malomed, B.A., Konotop, V.V., Lobanov, V., Torner, L.: Stabilization of solitons in bulk kerr media by dispersive coupling. *Opt Lett* **40** 1045 (2015).
- [80] Kartashov, Y.V., Konotop, V.V., Malomed, B.A.: Dark solitons in dual-core waveguides with dispersive coupling. *Opt. Lett.* **40** 4126 (2015).
- [81] Sakaguchi, H., Malomed, B.A.: One- and two-dimensional solitons in PT-symmetric systems emulating spin-orbit coupling. *New J Phys* **18**, 105005 (2016).
- [82] Huang, H., Lyu, L., Xie, M., Luo, W., Chen, Z., Luo, Z., Huang, C., Fu, S., Li, Y.: Spatiotemporal solitary modes in a twisted cylinder waveguide shell with the self-focusing kerr nonlinearity, *Commun Nonlinear Sci Numer Simulat* **67** 617 (2019).
- [83] Sakaguchi, H.: New models for multi-dimensional stable vortex solitons, *Frontiers of Physics*, **14**, 12301 (2019).
- [84] Huang, C., Ye, Y., Liu, S., He, H., Pang, W., Malomed, B.A., and Li, Y.: Excited states of two-dimensional solitons supported by spin-orbit coupling and field-induced dipole-dipole repulsion, *Phys. Rev. A* **97**, 013636 (2018).
- [85] Zhong, R., Chen, Z., Huang, C., Luo, Z., Tan, H., Malomed, B.A., Li, Y.: Self-trapping under two-dimensional spin-orbit coupling and spatially growing repulsive nonlinearity, *Frontiers of Physics*, **13**, 130311 (2018).
- [86] Kartashov, Y.V., Konotop, V.V., Zezyulin, D.A.: Bose-Einstein condensates with localized spin-orbit coupling: Soliton complexes and spinor dynamics, *Phys. Rev. A* **90**, 063621 (2014).
- [87] Li, Y., Zhang, X., Zhong, R., Luo, Z., Liu, B., Huang, C., Pang, W., and Malomed, B.A.: Two-dimensional composite solitons in Bose-Einstein condensates with spatially confined spin-orbit coupling, *Commun. Nonlinear Sci. Numer. Simulat.* **73**, 481(2019).
- [88] Ye, Z., Chen, Y., Zheng, Y., Chen, X., Liu, B.: Symmetry breaking of a matter-wave soliton in a double-well potential formed by spatially confined spin-orbit coupling, *Chaos, Solitons and Fractals* **130**, 109418 (2020).
- [89] Dai, C.Q., Zhou, G.Q., Chen, R.P., Lai, X.J., Zheng, J.: Vector multipole and vortex solitons in two-dimensional Kerr media, *Nonlinear Dyn* **88**, 2629 (2017).
- [90] Chin, C., Grimm, R., Julienne, P., and Tiesinga, E.: Feshbach resonances in ultracold gases, *Rev. Mod. Phys.* **82**, 1225 (2010).
- [91] Köhler, T., and Góral, K., Julienne, P., Production of cold molecules via magnetically tunable Feshbach resonances, *Rev. Mod. Phys.* **78**, 1311 (2006).
- [92] Inouye, S., Andrews, M.R., Stenger, J., Miesner, H.-J., Stamper-Kurn, D. M., and Ketterle, W.: Observation of Feshbach resonances in a Bose-Einstein condensate, *Nature*, **392**, 151 (1998).
- [93] Timmermans, E., Tommasini, P., Husseinb, M., Kerman, A.: Feshbach resonances in atomic Bose-Einstein condensates, *Phys. Rep.* **315**, 199 (1999).
- [94] Chiofalo, L.M., Succi, S., and Tosi, P.M.: Ground state of trapped interacting Bose-Einstein condensates by an explicit imaginary time algorithm, *Phys. Rev. E* **62**, 7438 (2000).
- [95] Yang, J., and Lakoba, T.I.: Accelerated imaginary-time evolution methods for the computation of solitary waves, *Stud. Appl. Math.* **120**, 265 (2008).
- [96] Sakaguchi, H., and Malomed, B.A.: Solitons in combined linear and nonlinear lattice potentials, *Phys. Rev. A* **81**, 013624 (2010).
- [97] Shchesnovich, V.S., and Doktorov, E.V.: Perturbation theory for solitons of the Manakov system, *Phys. Rev. E* **55**, 7626 (1997).